Complex Systems 1 (1987) 131–144

The Free Energy Concept in Cellular Automaton Models of Solid-Solid Phase Transitions

Daniel G. Maeder
Physics Section, University of Geneva,
CH-1211, Geneva 4, Switzerland

Abstract. Landau theories can describe characteristic features of shape memory alloys associated with their thermoelastic martensitic phase transformation. Such theories, based on a continuously variable free energy function $F(e,T)$, explain global behaviour satisfactorily but neglect microscopic aspects of the lattice change where the order parameter e can only switch between a few fixed values. In a corresponding *cellular* type theory, we replace the continuous $F(e,T)$ by a discrete set of functions F_j, each depending on continuous global variables such as temperature T and stress X. The processing algorithm minimizes for each cell the sum of F_j and the interface energies with its neighbours. At a fixed (T,X)-condition, this process is equivalent to a cellular automaton transition rule. The simple case of a 3-state, one-dimensional martensite model is discussed in detail; changes for two-dimensional extensions are outlined.

1. Introduction

The purpose of this paper is to present a new way of treating solid-solid phase transformations filling a gap between phenomenological, or Landau-type, and microscopic (based on lattice dynamics) theoretical descriptions. In our cellular automaton (CA) approach, the smallest element considered may contain a few hundred atoms and thus have essentially the properties of the bulk matter; all cells are identical, except that the presence of lattice defects may alter a few of them in such a way that they tend to change phase more easily than average cells. In fact, the introduction of *germ* cells is one of the essential features of cellular phase transition models, enabling detailed studies and simulations of nucleation processes.

The thermoelastic martensitic transformation of shape memory alloys, such as $Cu-Zn-Al$, is a particularly interesting candidate for CA models, because the origin of the characteristic surface patterns and their changes as a function of experimental conditions have been extensively studied by optical and electron microscopy [1]. The crystal structures of both the high-temperature "mother" (austenite or beta) and the low-temperature

© 1987 Complex Systems Publications, Inc.

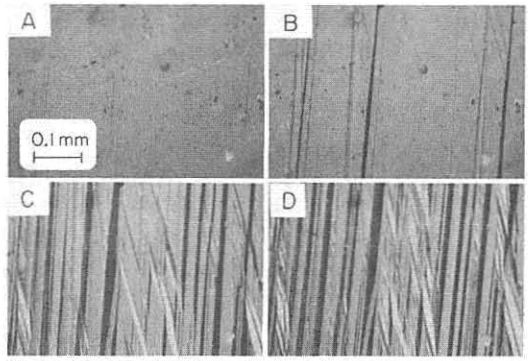

Figure 1: Photomicrographs of a $Cu-Zn-Al$ sample taken at various instants in a cooling period, showing the evolution of surface patterns from a few thin parallel platelets (a, at 17^0C,< 1%. of martensite) to the typical criss-cross of martensite variants (d, at 8^0C,> 90%m). Reproduced from [4].

"product" (martensite) phase are well known; the nucleation mechanism is still, however, a matter of disucssion among experts [2,3]. Transition dynamics, investigated recently by simultaneous observation of acoustic emission and changes in surface patterns [4,5], suggests an important role of submicroscopic nuclei whose stability depends on germ configurations and thermal cycling. The photomicrographs reproduced in figure 1 (from [4]) show typical patterns obtained at very low and at high martensite concentrations; the few thin parallel platelets in figure 1a could be represented by a two-state, one-dimensional cell model while the criss-cross of Figure 1d requires a two-dimensional model where each cell can assume several states representing either the austenite phase, or one of four self-accommodating martensite variants (called A, B, C, D in [1]).

Physically, the martensite variants are distinguished by the different orientations of the transformation strain tensor. This suggests a CA model in which the isotropic (or austensite) phase is represented by the zero cell state, and the different variants by cells in symmetric state pairs. Ideally, the CA simulation should produce output resembling directly the physical patterns seen under the microscope; figure 2 gives a hypothetical example showing the different orientations of interfaces in all martensite twins (AB, AC, etc.) as well as between the four martensite variants and austenite, following reference [1].

Figure 2 corresponds to an intermediate temperature; the CA must perform the transitions to "all austenite" or "all martensite" states at high and low temperatures, respectively. The particular pattern depends on the distribution of "germ" cells, and must approximately reproduce in successive thermal cycles. Furthermore, the model should respond to nonzero external

```
CD::::::::::::AA::::::::::::
CCD::::::::::AABD::::::::::
CCCD::::::::AABBDD::::::::::
:CCCD::::::AABB::DD::::::::
::CCCD::::AABBAC::DD::::::::
:::CCCD::AABBAACC::DD::::::
::::CCCD:ABBAAACCC::DD::::::
:::::CCCDBBAAAACCCC::DD:::::
::::::CCCCACDDDBBBB:::DD::::
:::::::CCC::CDDBBB:::::DD:::
::::::::CCC::CDBB:::::::DD::
:::::::::CCC::CB:::::::::DD:
::::::::::CCC::C::::::::::DD
```

Figure 2: Evolution of a one-dimensional cellular automaton model for a shape memory alloy. : represents cells of atoms in the high-temperature austenite phase; A, B etc. represent four variants of the low-temperature martensitic phase. The evolution starts at the top of the figure, with "germs" of the martensitic phase, and follows dynamics appropriate for an intermediate temperature.

stress components by changing the equilibrium between A, B, C, D cells.

To explain how the CA rules for such models are constructed, it is sufficient to chose a simplified example using only three cell states, say (A, O, B). In this paper, the case of a one-dimensional lattice is fully discussed, in close analogy with a phenomenological description; extensions to the two-dimensional case will be outlined, but details are left to a forthcoming paper [6].

2. Phenomenological Theories

Falk [7] briefly reviews applications of Landau-type theories and shows that even a one-dimensional model of this kind explains global behaviour of martensites quite satisfactorily, although microscopic aspects (phase boundaries) are neglected. The so-called order parameter denoted e is an internal variable of the system which characterizes the progress of the transition. It is not necessarily related with ordering phenomena; in the case of martensitic transformations, it is a mechanical strain which varies between zero (in the high-temperature, or austenitic phase) and either of two finite values $\pm e_1$ in the martensitic phase.

The thermodynamics of the system is fully determined by a free energy density function f which depends only on e and the temperature T. Under the influence of an external stress σ, the total free energy density becomes

$$F_\sigma(e, T) = f(e, T) - \sigma e. \tag{2.1}$$

In thermal and mechanical equilibrium, e will adjust itself so that $F_\sigma(e, T)$

is minimized while the internal stress response

$$\sigma(e,T) = \partial f(e,T)/\partial e \tag{2.2}$$

balances the external stress. Landau expanded $f(e,T)$ into a power series in e which he cut off after the fourth power; for symmetry reasons, in the martensitic transition, odd powers are absent so that $f(e,T)$ can be written as

$$f(e,T) = f_0 + Ae^2 + Be^4 \tag{2.3}$$

where f_0, A and B are analytic functions of the temperature T. In order to obtain for $f(e,T)$ a single minimum (located at $e = 0$) at high temperature, and two symmetric minima for $T < T_0$, the simplest possibility is to assume B to be a positive constant and to let A change sign at T_0 by putting $A = (T - T_0)$. For the purpose of studying the evolution of e at any fixed temperature, we may drop the "constant" term f_0. Furthermore, we can simplify later formulas by using an *ad hoc* temperature scale (in which $T_0 \equiv 0$), as well as suitable order parameter and stress units so that the free energy expression becomes

$$F_{\text{Landau}} = -\sigma e + Te^2 + Be^4. \tag{2.4}$$

Setting its dervative equal to zero produces a cubic equation for determining equilibrium values for e

$$e(2Be^2 + T) = \sigma/2. \tag{2.5}$$

From the solutions of (2.5), it is evident that, for a vanishing external stress field, the Landau ansatz describes a second-order temperature-induced phase transition at $T = 0$ which has *no* hysteresis. On the other hand, at negative temperatures, external stress can induce a first-order phase transition associated *with* hysteresis.

By adding a sixth power term to the free energy expression, one obtains:

$$F_{\text{Devonshire}} = \sigma e + Te^2 - Be^4 + Ce^6. \tag{2.6}$$

The added complexity leads to the existence of a critical point given by

$$T_c = 15\,C\,ec^4, \quad e_c = \sqrt{B/5C}, \quad \sigma_c = 16\,C\,e_c{}^5 \tag{2.7}$$

above which there are no phase transitions. Below σ_c, there is a first-order temperature-induced phase transition with hysteresis; the stress-induced phase transitions are also of the first order. Equilibrium values of e derived from (2.6), plotted in Figure 3 as a function of temperature, show the thermal hysteresis. Similar plots as a function of external stress for different temperatures in Figure 4 demonstrate the shape memory effect.

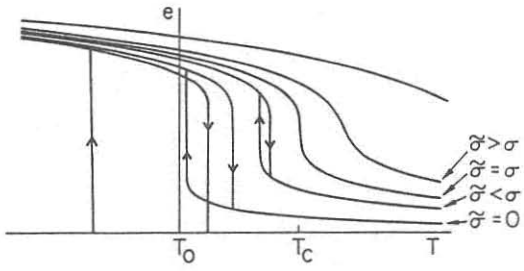

Figure 3: Thermal hysteresis: equilibrium order parameter (Devonshire theory) as a function of temperature for different values of external stress (after Falk [7]).

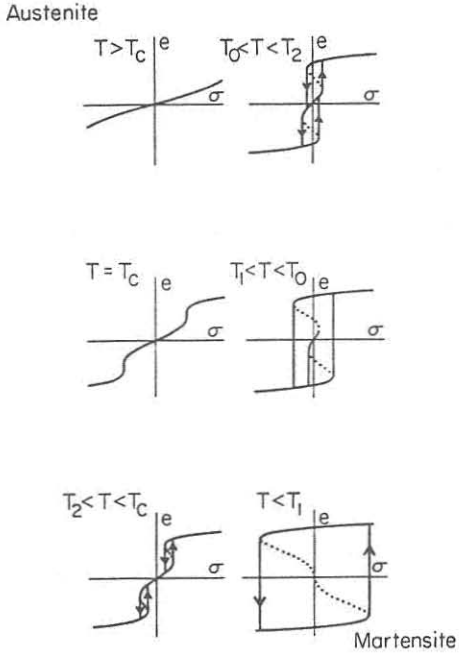

Figure 4: Mechanical hysteresis: equilibrium order parameter (Devonshire theory) as a function of external stress for different temperature values. Rearranged from Falk [7].

3. Basic notations for a one-dimensional cellular model

3.1 Cell states

Phenomenological theories use a single order parameter which may evolve continuously, except for partial jumps over a certain range, from near zero at high temperature to large positive and negative values at low temperature. In contrast, cells are assumed to exist only in a few distinct states, associated with well-defined strains via a numerical state variable S:

$A \rightarrow S$	$-1 \rightarrow e =$	$-e_1$
:	0	0
B	1	$+e_1$

State values of individual cells are denoted S_j, with index $j = 1...C_tot >> 1$. Except for interface regions (which could in a more elaborate model be represented by intermediate states, a, b, with reduced strain), most of the cells have strains not very different from the nominal values, 0 or $\pm e_1$. Assuming linear strain superposition along the array of cells, the sum

$$e = e_1 \sum_{j=1}^{C_{tot}} \frac{S_j}{C_{tot}} \tag{3.1}$$

would be the direct analog of the phenomenological order parameter. However, it is evident that the cell system can be completely martensitic and still have $e \approx 0$, contrary to phenomenological models which neglect the possibility of strain cancellation in actual domain patterns (Figure 1).

3.2 System state variables

As expression (1) does not necessarily tell to which degree the system is transformed, at least one more system variable is required in the equation for the free energy. The simplest choice is the martensitic fraction

$$m = \sum_{j=1}^{C_{tot}} \frac{|S_j|}{C_{max}} = \frac{(\mathrm{Sum}_A + \mathrm{Sum}_B)}{C_{tot}}; \quad 0 \leq m \leq 1. \tag{3.2}$$

The e parameter is retained, but simplified by putting $e_1 \equiv 1$ and rewriting it in the form

$$e = \frac{(\mathrm{Sum}_B - \mathrm{Sum}_A)}{C_{tot}}; \quad -1 \leq e \leq 1 \tag{3.3}$$

which suggests obvious extensions to 2D-models (see 3.3).

3.3 Driving forces

External variables used in the free energy ansatz (6) are the stress, σ and the temperature, T. Since e will now be replaced by $S_j = 0, \pm 1$, the remaining

terms (B, C) are simply multiplied by $|S_j|$, just like the temperature; they can therefore be omitted if the temperature scale is shifted by a suitable constant. Thus, the free energy becomes the sum of two driving terms, the first of which acts on the sign of e ($\sigma < 0$ favors transitions to the A state) while the second one acts on m ($T < 0$ tends to increase the number of both A and B states).

On the other hand, the elastic reaction of progressing martensitic domains upon the remaining material will set up *internal* forces, one opposing σ and one opposing T. First, imagine that the sample is clamped, so that A and B states should form in equal amounts in order to maintain constant sample length; if their numbers differ, this will set up internal stress $e \cdot U$, with an unbalance factor U related to the material's elastic constants and clamping conditions. By adding this internal bias to σ, we define

$$X = \sigma + e \cdot U, \quad U \geq 0 \tag{3.4}$$

an effective stress to be used in computing the free energy. A two-dimensional model is subject to more complex elastic reactions, involving at least three martensitic variants; in the most general case σ and e have three components each, acting on the B/A, and D/C, and the CD/AB variant ratio respectively.

Secondly, A and B states may, in addition, have a common strain which cannot cancel out, except by creating other variants like C and D that would not fit into our simplified model. Thus, an increasing total of martensitic cells sets up another internal stress component, opposing any further transitions just as if a temperature higher than the true physical temperature had been inserted into $F(S_j)$. We therefore define a temperature shift $m \cdot W$, where W reminds one of some relation to the width of the transformation range (M_s is martensite start, M_f is martensite finish). From now on

$$T = \text{physical temperature} + m \cdot W, \; W \geq 0 \tag{3.5}$$

denotes an effective temperature to be used in the free energy expression

$$F(S_j) = -X S_j + T |S_j|. \tag{3.6}$$

$F(Sj)$ thus represents the free energy of one cell in state Sj, subject to an effective stress X and an effective temperature T but assumed to be isolated against direct interactions with its neighbors. Neighborhood configuration energy values must be added to F(Sj) in order to construct CA rules that will minimize the total free energy (see section 4). X and T are the same for all cells but depend crucially on the total numbers of cells in the different states, for example, equilibrium temperatures for $m \approx 0$ and $m \approx 1$ (start and end of the transofmration) would differ by the value of W if W was a constant (see section 5 for a better-fitting assumption).

3.4 Interface parameters

The elastic energy of a pair of adjacent cells in various states is assumed to be independent of X, T and symmetric under A, B interchange. For

code	Config.	$S=-1$	$S=0$	$S=1$
-4	A?A	$2E_A=-2$	$2E_0=6$	$2E_B=2$
$-3-1$	A?:	$E_A+E_0=2$	$E_0=3$	$E_B+E_A=4$
$-2,2$	A?B	$E_A+E_B=0$	$2E_0=6$	$E_B+E_A=6$
0	:?:	$2E_0=6$	0	$2E_0=6$
1,3	B?:	$E_B+E_0=4$	$E_0=3$	$E_A+E_0=2$
4	B?B	$2E_B=2$	$2E_0=6$	$2E_A=-2$

Table 1: Interface energies with typical numerical values for cells.

simplicity, let us assume linearity so that they can be added for all neighbors of a given cell. Using the austenitic state as a free energy reference implies $E_0 \equiv 0$ (for :: pairs), and there are only three other kinds of pairs to consider for (possibly nonzero) interface energies, namely, for example:

$:\mathtt{A}, :\mathtt{B}, \mathtt{A}:, \mathtt{B}: \rightarrow E=$	$E_0=$	3
AB, BA	E_B	1
AA, BB	E_A	-1.

To assemble the interface energy of a cell in state S having two neighbors in states L, R (left and right) into a lookup table, we use as the main argument a neighborhood code defined as code $= L + 3 \cdot R$, and obtain the results in table 1.

3.5 Germ cells

There must be at least one A or B germ so that slow growth of martensitic regions can be performed by this model; otherwise the system would have to be supercooled until the condition for spontaneous nucleation was satisfied simultaneously at all sites. Inversely there must be one : germ to avoid superheating of a completely martensitic array causing spontaneous back transformation everywhere. 2-D models may contain several germs of either kind, allowing a great variety of reproducible patterns.

The simplest method to assure the presence of germs is to forbid their processing once they have been initialized. Alternatively they may be treated during each time step like any other cell, but must be "refreshed" to their predefined state periodically.

4. The CA transition rule

For cell j, processing consists of evaluating $F(S)$ + table[code(j), S] for the three possibilities of S, using the code for the given neighborhood at that site; the one producing the lowest sum is then adopted as the new S_j value, except when this would change S_j by more than one unit (tunneling between A and B states is forbidden). More explicitly, the two or three

total free energy values to choose from can be written as:

$$\begin{aligned}\texttt{if old } S_j = \quad -1,0 \to E_- &= X + T + \texttt{table}[S(j-1) + 3 \cdot S(j+1), -1] \\ -1,0,1 \to E_0 &= \texttt{table}[S(j-1) + 3 \cdot S(j+1), 0] \\ 0,1 \to E_+ &= X + T + \texttt{table}[S(j-1) + 3 \cdot S(j+1), 0]\end{aligned}$$

It is straightforward to verify that the minimizing transition is achieved by the following Pascal-style program using the numerical table values: BEGIN RULE:=OLD; (NO CHANGE, except in the following CASES).

```
   CASE CODE OF

-4 :  BEGIN
         IF (OLD=0)  AND (T<6+ABS(2-X)) THEN RULE:=SGN(X-2);
         IF (OLD=-1) AND (T>8-X)        THEN RULE:=0;
         IF (OLD= 1) AND (T>4+X)        THEN RULE:=0  END;
-3,-1 : BEGIN
         IF (OLD=0)  AND (T<ABS(1-X))   THEN RULE:=SGN(X-1);
         IF (OLD=-1) AND (T>1-X)        THEN RULE:=0;
         IF (OLD= 1) AND (T>X+1)        THEN RULE:=0  END;
-2,2 :  BEGIN
         IF (OLD=0)  AND (T<6+ABS(X))   THEN RULE:=SGN(X);
         IF (OLD=-1) AND (T>6-X)        THEN RULE:=0;
         IF (OLD= 1) AND (T>6+X)        THEN RULE:=0  END;
0 :     BEGIN
         IF (OLD=0)  AND (T<ABS(X)-6)   THEN RULE:=SGN(X);
         IF (OLD=-1) AND (T>-6-X)       THEN RULE:=0;
         IF (OLD= 1) AND (T>-6+X)       THEN RULE:=0  END;
1,3 :   BEGIN
         IF (OLD=0)  AND (T<ABS(1+X))   THEN RULE:=SGN(X+1);
         IF (OLD=-1) AND (T>-1-X)       THEN RULE:=0;
         IF (OLD= 1) AND (T> 1+X)       THEN RULE:=0  END;
1,3 :   BEGIN
         IF (OLD=0)  AND (T<6+ABS(2+X)) THEN RULE:=SGN(X+2);
         IF (OLD=-1) AND (T> 4-X)       THEN RULE:=0;
         IF (OLD= 1) AND (T> 8+X)       THEN RULE:=0  END;
END; (of CODE cases)
END; (of RULE function)
```

For all practical purposes, both X and T can be considered as slowly varying parameters so that this rule becomes a fixed logical CA table; however, when any of the driving forces (including m or e) changes appreciably, the CA table has to be recalculated.

5. Results

As special CA hardware was not available for the present work, numerical model testing was limited either to the one-dimensional case (with a

number of cells arbitrarily fixed to $C_max = 201$ using about two-thirds of a PC graphics screen for displaying results), or to relatively small two-dimensional arrays (e.g., 25 rows × 50 columns displayed in color text mode). On the other hand, the necessity of implementing the rules by conventional programming gave us full flexibility for deviations from an orthodox CA concept; e.g. by introducing randomness into the process, or using special conditions at boundaries, or different updating modes. The type of CA rule adopted in this paper allows a certain temperature range where an oscillatory regime would invade the whole system if the processing was done in the orthodox CA mode (all cells are updated quasi-simultaneously). While such a regime might be looked at as a crude model of soft-zone vibrations postulated by some authors discussing the martensitic nucleation mechanism [2], its :A:A:A structure implies an unrealistic increase of free energy. In the "even-odd mode" all even-numbered cells are updated in one step leaving the odd cells unchanged; in the following step, all odd-numbered cells are updated, and so forth. This updating mode has proved fully efficient to eliminate unphysical checkerboard structures but is still compatible with soft-zone vibration effects in the immediate neighborhood of germ cells. The "random scanning mode" where cells are updated at random and their new states immediately used for further processing of neighbords produces generally similar results except that periodicities disappear. In simulating thermal and/or mechanical transofmration cycles, the rule program remained unchanged but the parameters T and X were recalculated after each CA step.

Some properties of the model can be directly derived from the rules, in particular the conventional transition temperatures M_s, M_f, A_f, and the hysteresis expressed by the well-known experimental relations:

$$A_s > M_f; \quad A_f > M_s. \tag{5.1}$$

Normal growth or shrinking of martensitic regions is governed by the rule for the transition A :: ⟷ AA :; at zero stress, there is an equilibrium temperature at

$$T_{\text{forward}} = T_{\text{backward}} = -E_A - m \cdot W. \tag{5.2}$$

In particular, at $m \approx 0$ this gives $M_s = A_f = -E_A$ (+1 in the numerical example), and at $m \approx 1$ this gives $M_f = A_s = -E_A - W$. Unless an additional term is introduced, this simplified model has no hysteresis. The evident solution of this problem is a friction term which leaves T_{forward} unchanged but increases T_{backward} (e.g. by one temperature unit, which corresponds about to $A_f - M_s$). The much larger hysteresis at high m can be explained by assuming:

$$W = W_o(1 - k \cdot m), \quad W_o > 0, 0 < K \leq 1 \tag{5.3}$$

If, for simplicity, we use $k = 1$, $m \cdot W$ is a maximum at $m = 0.5$ but drops to 0 at $m = 1$. In that case the model predicts a variable hysteresis depending

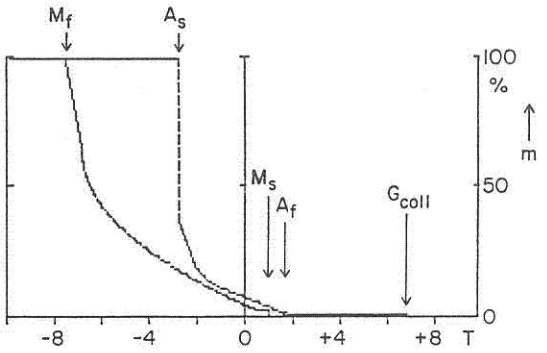

Figure 5: Thermal hysteresis at zero applied stress in the one-dimensional model with 201 cells (4000 time steps). To be compared with figure 3.

on the depth of the transformation cycle; in the extreme (when m reached 100%)

$$M_f = M_s - W_0/4, \qquad A_s = A_f \tag{5.4}$$

The thermal hysteresis curve shown in figure 5 was obtained with $Wo = 25$, $k = 0.8$ and friction$= 1$. It resembles to some of the e curves in figure 3 although we did not plot the order parameter (which remained ≈ 0 in the absence of external stress, $X = 0$), but rather the martensite fraction m. In addition to M_s, M_f, A_s, A_f, a new transition temperature called G_{coll} (germ collapse) is seen at about +7 temperature units. The germ consisted in this experiment of an A??B pair separated by two normal cells; it was processed in an even-odd mode but would be restored before the following time step would start. In even steps, the direct neighbor of the A germ would not be processed and therefore could not disappear; the same is true in odd-time steps for the neighbor of the B germ. Thus the martensitic bridge originating from this germ pair is somewhat fragile but nevertheless more stable than a single-variant region shrinking back from austenite according to [14]. If there was no germ in the whole array, the only transition to martensite would follow the rule ::: $\rightarrow$: A :; at zero stress, this requires supercooling to $T_{\text{spont.mart.}} = -2E_0$ or -6 units (may coincide with M_f).

Inversely, in the absence of any austenite germ, back transformation could occur according to two processes, AAA $\rightarrow$ A : A or AAB $\rightarrow$ A : B depending on the presence of a twin boundary; the latter can be broken up by applying a sufficiently strong external stress as seen by comparing the respective temperatures

$$\begin{aligned} T_{\text{spont.aust.}} &= 2(E_0 - E_A), && \text{or } +8 \text{ units} \\ T_{\text{twinbreak}} &= 2E_0 - E_A - E_B - |X|, && \text{or } < 6 \text{ units.} \end{aligned} \tag{5.5}$$

Whether twins were formed during the cooling depends on the germ config-

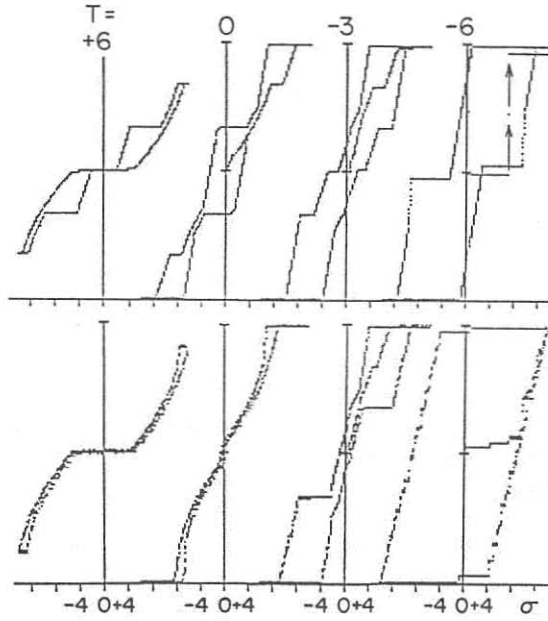

Figure 6: Mechanical hysteresis at different temperatures in one-dimensional model with 201 cells. Upper row is obtained by strict CA processing (in even-odd mode) to avoid the formation of checkerboard regions, lower row by random scanning. To be compared with Figure 4.

uration and the unbalance paramter U. Using $U = 5$, one A??B and one A?B martensite germ, and austenite germs on either array end, stress cycling produced the strain loops shown in Figure 6 which are directly comparable to those in Figure 4 (e plotted against stress in both cases). With standard CA processing the shape memory effect sets in $T = -6$ units. The peculiar shape of the loops (which depends on the particular choice and position of the two germ pairs) prompted us to repeat the experiment in the random scanning mode. The smoothing effect of this processing mode is evident, and the shape memory works already at $T = -4$ units.

6. Outlook

So far, the model has been tested for small arrays only, using conventional programming on a small computer. The one-dimensional case has been explored to some extent and revealed its particularities as far as the origin of hysteresis and the role of germ pairs is concerned. The even-odd processing mode not only proved useful in solving the checkerboard problem in CA but also provided a method for creating germ configurations with different nucleation potential and stability against heating.

Tentative studies on two-dimensional versions have shown that hysteresis increases with the number of neighbor interactions, without a necessity for introducing *ad hoc* terms as in the one-dimensional model. Still with three states, three more parameters would be required since horizontal and vertical pairs should have different interactions; on the other hand, a two-dimensional model allows a very rich variety of martensite-like patterns to be created. The rules are not essentially different from those presented above, except for a larger number of parameters and more voluminous lookup tables. Preliminary results are reported in a forthcoming paper [6].

As the algorithm which minimizes the local free energy can be expanded into a deterministic lookup table of the kind required by CAMs such as Toffoli's parallel processing CA machine [8], fast simulations of martensitic transformations on a large two-dimensional array appear quite feasible. We expect that in future work using a CAM, the gain in processing speed will allow us a finer adjustment of model parameters on the basis of observed transformation patterns. Ultimately this should lead to a valid four-variant martensite model which might be close to the physical reality.

References

[1] T. Saburi and C.M. Wayman, *Acta Metallurgica*, **27** (1979), 979.

[2] G. Guenin and P.F. Gobin, *Metallurgical Transactions*, **13A** (1982), 1127-34.

[3] G.B. Olson and M. Cohen, "Dislocation Theory of Martensitic Transformations," *Dislocations in Solids*, **7**, edited by F.R.N. Nabarro (North-Holland).

[4] A. Steiner, "Etude de la transformation martensite $\beta \rightarrow \beta'$ dans le $Cu - Zn - Al$ par la methode des emissions acoustiques", PhD thesis No. 2180, Geneva University, 1986.

[5] R. Gotthardt, D.G. Meader, and A. Steiner, "Relationship Between Shape Memory Effect, Nucleation and Acoustic Emission in Cu-Zn-Al," presented at SMA '86, Sept. 6-9, 1986 at GUILIN (c/o The Nonferrous Metals Society of China).

[6] M. Droz and D.G. Meader, "Cellular Automata Approach to the Dynamics of Martensitic Transformations," presented at ICOMAT '86 on August 26-30, 1986 at NARA (c/o The Japan Institute of Metals).

[7] F. Falk, "Acta Metallurgica", **28** (1980), 1773-80; Journal de Physics, C4-3, supplements 12/43 (1982).

[8] T. Toffoli, *Physica*, **10D** (1984), 195.